Bending Load Response of Mechanical Butt Joints in Composite Materials: A Comprehensive Study

Ali Can*1, Mert Yildiz 1
* Department of Mechanical Engineering, Faculty of Engineering,
Pamukkale University, Kinikli 20070 Denizli, Turkey

ABSTRACT

In this study, the load-carrying capacities of the mechanical butt joints have been obtained experimentally and numerically under three point bending load. Composite plates have been jointed as a mechanical butt joint with the jointing element. The shape of I profile has been used as the geometric jointing element throughout the study. It has been determined that the results obtained from the Abaqus finite elements program and the data obtained from the experiment support each other. According to the investigation optimum jointing parameters have been found with the h/2w ratio of 0.5, b/w ratio of 0.5 and z/b ratio of 0.5. It has been concluded that considering that the first damage will occur on the jointing element with profile I before the jointed composite specimens and consequently composite structures are totally damaged, jointed composite structures can be made to work longer through the repairment of the jointing element.

KEYWORDS: Three point bending; Butt joints; Failure analysis.

I. INTRODUCTION

The structures made up of composite materials are usually subjected to static and dynamic loadings. Because of different designs or productions, these structures may be made up of one or more joints. The purpose in doing so is to fulfill the transfer of force from the main structure. The biggest problem in the composite structures is that there appears damage on the joint zones of the materials in system [1]. The damage in these joint zones leads to the fall in strength. Because of the weakness in the joint zones, there are a lot of joint methods available in literature. According to the literature review, most of the research has been determined to have been done over the joint variety [2-10]. El Mahi and Bezazi [11] carried out an experimental work to determine the flexural behaviour of two types of cross-ply laminates, glass-fiber/epoxy laminates and hybrid glass-fibre/Kevlar-fibre/epoxy laminates under fatigue load. Megueni et al. [12] carried out a finite element method to analyse the evolution of the stress intensity factor for cracks repaired with bonded hygrothermal aged composite patches. Choi [13] investigated a failure area method to predict failure loads of mechanically-fastened composite joints under plane stress condition. Altan et al. [14] designed an experimentally and numerically study to analyze the load-carrying capacities of composite structures connected face-to-face by a butterfly coupling component without adhesive. They also supported the results of the experimental studies with numerical analysis. Kumar et al. [15] carried out analytical and experimental analyses of composite epoxy adhesive joints. They also made comparison between the experimental and theoretical stresses. Kim et al. [16] carried out an experimental study on the effect of overlap length on the failure of composite-to-aluminum single-lap bonded joints. They tested carbon composite-to-aluminum single-lap adhesive joints with six different bonding lengths under tension. Seo et al. [17] used the epoxy-based adhesive metal butt joints to evaluate the strength and failure probability. They conducted the conventional test methods such as tensile, shear and four-point bending tests to evaluate the probability distribution of adhesive strength. Nader et al. [18] investigated the size effects associated with length and width, on the bending strength of marine grade polymer matrix laminated composites. And they developed a new expression for predicting the strength size effect. Dawood et al. [19] conducted to evaluate the two-way bending behaviour of 3-D glass fiber reinforced polymer sandwich panels. Khalili et al. [20] studied experimentally the effect of reinforcements in the adhesive layer using a single lap joint with composite adherents. Roy et al. [21] conducted an experimental study of the initiation and development of damage in composite/composite joints. Basturk and Tanoglu [22] determined the flexural behaviours of the sandwich structures composed of Al foams and FMLs with three point bending test configuration. Radhakrishnan et al. [23] investigated the performance of flanged panel bolted joints used in Glass Reinforced Plastic (GRP) sectional tanks using a combination of experimental and computational methods.

Within this study, mechanical jointing elements with I geometric shape instead of the method of bonding have been used. Therefore the purpose of this study is to analyze the mechanical behaviours of the specimens jointed mechanical butt with I profile jointing element in different geometry by three point bending test at laboratory. Moreover, the analysis of the specimen models with the finite elements method will be realized three dimensionally with ABAQUS package program. The main purpose is to determine the I profile lock jointing element with the optimum geometry by enabling the support of the results that will be obtained in an experimental method by the finite elements program ABAQUS.

II. MATERIALS AND METHODS

The manufacturing of the glass fiber/epoxy composite material used in this study was conducted with the composite material-manufacturing press in our department's laboratory, as seen in Figure 1.

Fig. 1: Composite material-manufacturing press.

It was decided according to the data from the finite elements program Abaqus and literature reviews that composite plates should be manufactured as glass fiber sequence $[0/90]_{2s}$ and the plates were manufactured according to this order. The manufactured composite plates were shown in Figure 2.

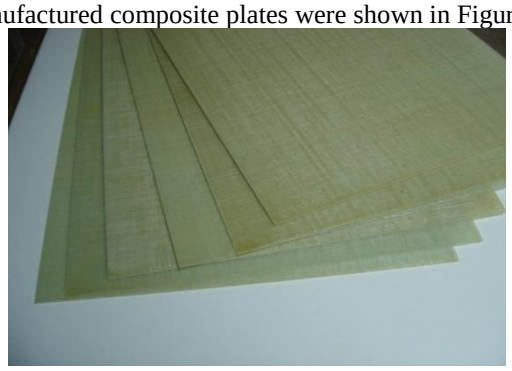

Fig. 2: Manufactured composite plates.

Epoxy for the matrix material contains a mixture of 100/80 Ciba Geigy, Bisphenol A, CY-225 epoxy and Ciba Geigy, Anhydride, HY-225 hardener. The entire specimens used in this study were cut at the Kardesler Glass Firm with the water jet from the composite plates manufactured according to the prescribed geometric parameters (Figure 3). With the use of water jet for the cutting, the potential cutting errors on the specimen were eliminated.

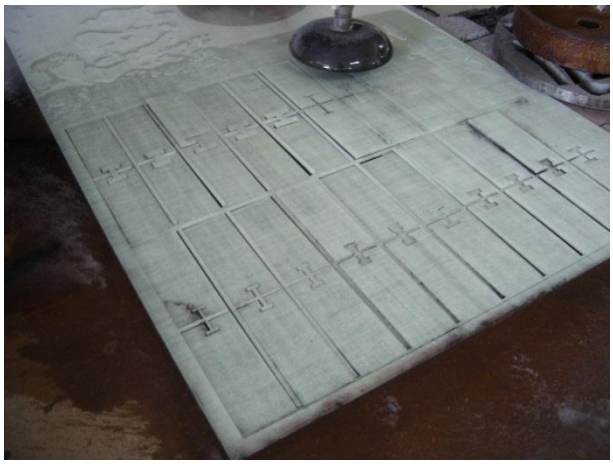

Fig. 3: Specimen cutting with water jet.

Firstly, the volume ratios of the manufactured glass fiber-epoxy composite plate were determined and then their densities were found. For this, the glass fibers used as the fiber material were weighed before the manufacturing of the composite plate. The weight of the matrix material was calculated by extracting the weight of the fiber material from the total weight of the manufactured composite plate.
The mechanical properties of the glass fiber-epoxy composite material under tensile, compression and shearing loads were determined according to ASTM standards. As the composite plate was made up of one-way woven glass fiber clothes, their mechanical properties change in two different ways. The fiber direction was accepted as (1) direction and the direction perpendicular to the fiber was taken as (2) direction. The mechanical properties of the composite plate on 1-2 planes were obtained by using three specimens for each mechanical property and average properties were obtained. Samples from the specimen required for the determination of the mechanical properties are shown in Figure 4.

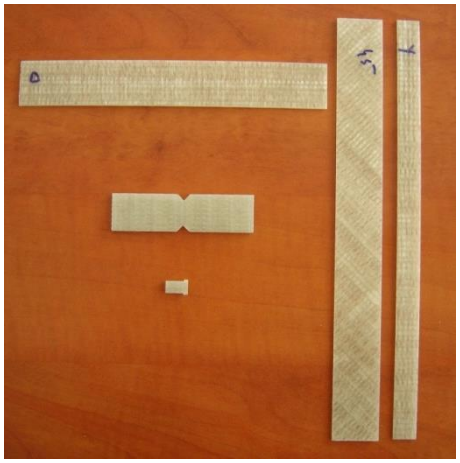

Fig. 4: Specimens required for the determination of the mechanical properties.

The experiments conducted for the mechanical properties to be determined were made at 23±1°C room temperature and under %50±10 relative humidity according to the ASTM standards. The experiments were made with Instron 8801 instrument having the capacity of 50 kN load. Strains were determined with two-way video extensometer as shown in Figure 5. Video extensometer determines the strains with no contact the surfaces of the specimen. Dots are marked on the specimen towards 1 and 2 by the use of a special marking pen and video extensometer helps to determine how much the distance between these dots stretch or contract during the experiment. The amount of stretching and contracting can make it possible to determine the strain of that material towards those directions.

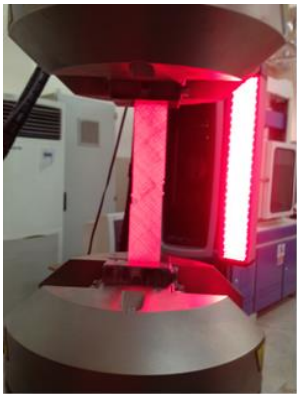

Fig. 5: Experiment with video extensometer.

The mechanical properties of the composite material obtained from the experiments under room conditions are given in Table 1.

Table 1. Mechanical properties of the composite material

E_1 (MPa)	E_2 (MPa)	G_{12} (MPa)	ν_{12}	X_t (MPa)	Y_t (MPa)	X_c (MPa)	Y_c (MPa)	S (MPa)
41600	11000	2900	0.20	772	80	290	75	85

Experimental and Optimization Procedure

Three-point bending experiment is the most commonly used of the bending tests. The basic principle of the experiment is that it accepts the material used as the beam model. As the beam equation is derived according to the ideal moment status, the shear stress on the beam is required to be at a negligible level when compared with the normal stresses. While the experiment specimen is horizontally placed on the supports lengthways, load is exerted on it just in the middle. The schematic presentation of the three-point bending experiment is given in Figure 6.

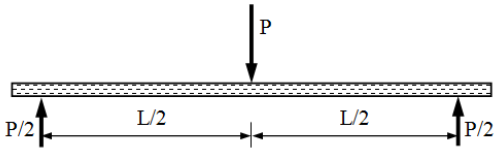

Fig.6: Three-point bending.

The three-point bending apparatus to be used in the experiments has been designed and manufactured according to the ASTM D 790-D 6272 standards. The three-point bending apparatus being currently manufactured is shown in Figure 7. The experiments conducted were done by using the experiment apparatus designed by us.

Fig. 7: Manufactured three-point bending apparatus

Jointed mechanical butt model made with the jointing element whose geometric dimension optimization will be made is given in Figure 8. Composite plates have been manufactured as glass fiber sequence $[0/90]_{2s.}$ To join the composite plates butt to butt, close-fit method has been used. Tolerance for the close-fit method has been taken as 3%. The thickness and material of the jointing lock have been taken as the same as the thickness and material of the semi specimen. In the experimental study to be conducted, the exact length of the specimen has been taken as 200 mm and their width as W= 40mm. Because the jointing element is jointed with a locking between two semi specimens, it is called the lock jointing element. Accordingly, the load-carrying capacity of the jointing element has been taken as joint or damage load. To analyze the effects of different measurement values, the values of b/W, z/b and h/2W ratios have been changed between 0.3 with 0.7. Here, is the ratio of lock width to the width of semi specimen (b/W), is the ratio of lock middle/end width to the lock width (z/b) and is the ratio lock length to the semi specimen width (h/2W). The end and middle width of the lock jointing element has been shown with z, its length or height with h and its width with b.

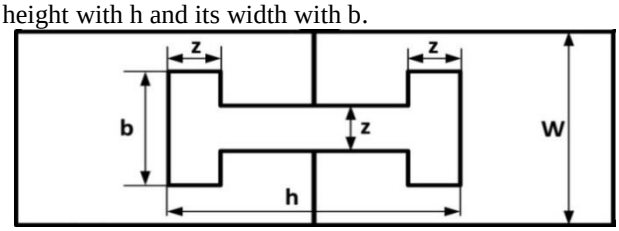

Fig. 8: Dimensions of the jointing element with profile I.

In Table 2, the dimensions for the I profile lock jointing element geometry are given. With the values in the table, I profile lock jointing elements have been made in different dimensions. However, because the geometric form required for locking with the semi specimen with the jointing element's z widening dimensions did not occur, no manufacturing was made at some ratios. Consequently, optimization was realized at all the ratios where the manufacturing was possible.

Table 2. Dimension for the I profile lock jointing element geometry

Dimension ratios		*b/W*					**Dimension (mm)**
		0.3	***0.4***	***0.5***	***0.6***	***0.7***	
		12	16	20	24	28	**b**
z/b	***0.3***	3.6	4.8	6	7.2	8.4	**z**
	0.4	4.8	6.4	8	9.6	11.2	
	0.5	6	8	10	12	14	
	0.6	7.2	9.6	12	14.4	16.8	
	0.7	8.4	11.2	14	16.8	19.6	
h/2W	***0.3***	24					**h**
	0.5	40					
	0.7	56					

Numerical optimization was conducted by using the analysis results made with the finite elements method. Abaqus 6.11 was used in the numerical analysis made with the finite elements method. To compare the stress distributions occurring on the joints in various geometries, stresses were taken on the lock (Way 1 and Way 2) as shown in Figure 9. In the analyses made, bending load value was taken as 30 N/mm^3 body force. The stress values obtained from the stress analyses made under the same load were obtained different because of the different z/b ratios. Viewed in general, the maximum stresses were observed on the lock jointing element.

The stress results of the analysis conducted by using the finite elements method were acquired as numerical value and color distribution on the whole composite structure, and stress-normalized stress way graphics were made so that the stress variations of the jointed butt composite specimens could be analyzed. In the following stages of the analysis, the stress distributions obtained and were analyzed and the aim was to determine the specimen with the highest load-carrying capacity.

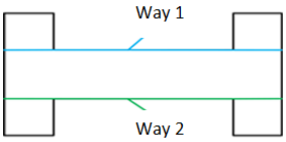

Fig.9: Stresses on the lock (Way 1 and Way 2).

A number of failure theories have been put forward to determine the damage load numerically and to model the occurrence form of the damage. The principal purpose of these theories is to determine in advance the stresses at which materials will be damaged, thus determining the loading limits. This study was intended, by using the Hashin failure theory, to find out where the first damage occurred and to determine the force that led to this damage. Hashin criteria divides the damage into modes and analyzes each according to compression-tensile and stress-strain cases separately. Therefore, Hashin criteria can enable us to understand easily whether the damage on the composite material is caused by the matrix, fiber or separation of the layers.

III. RESULTS AND DISCUSSION

Experimental optimization of the jointing element

Three-point bending experiments were conducted on Instron 8801 instrument having the capacity of 50 kN load as shown in Figure 10. All the specimens were loaded at a fixed jaw speed of 1 mm/min. For each model, joint (damage) load- lock displacement graphics were drawn. The moment any fall was observed in the load applied, the experiment was ended. The damage load on the specimen occurred in the first fall in the load applied.

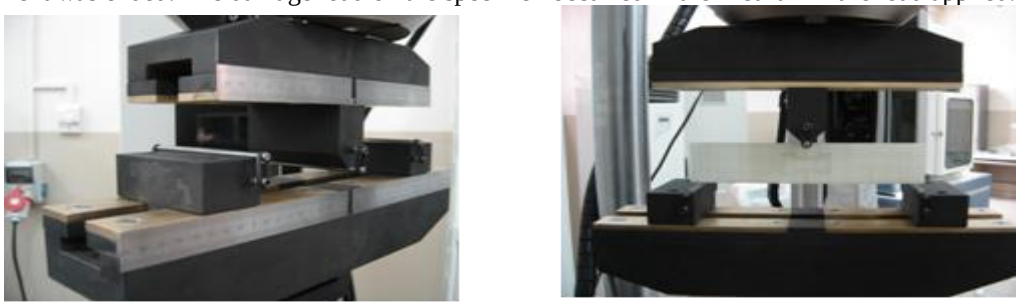

Fig. 10: Three-point bending experiment.

When the applied load reached the damage load, damage ruptures started to occur either on the composite lock or on the composite structure around the lock. To understand the shapes of the damage, the experiments of some specimen were continued till their last damage. Thus, the effects of lock geometry were analyzed.
The load-carrying capacities of the specimen made with the jointing elements of different (h/2W) ratios according to (z/b) ratios are shown in Figure 11. As seen in the figures, load-carrying capacity largely depends on (z/b) and (b/W) ratios. When (h/2W) ratio is 0.5 and 0.7, the load-carrying capacities of the locked specimen have been found as higher than the other dimensions and as almost the same. The joint load values obtained when (h/2W) ratio was 0.5 and 0.7 and especially (z/b) ratio was 0.5 are extremely high. Considering the joint loads from the aspect of (b/W) ratio, it was obtained as the maximum at the values of 0.5 and 0.6. This case changes due to the cross-section change when (h/2W) ratio is 0.3. According to the results of the experiment conducted, when (h/2W) ratio was 0.3, maximum joint load was achieved when (b/W) ratio was 0.3 and (z/b) ratio was 0.4. When (h/2W) ratio was 0.5, maximum joint load was achieved when (b/W) ratio was 0.5 and (z/b) ratio was 0.5. When (h/2W) ratio was 0.7, maximum joint load was achieved when (b/W) ratio was 0.6 and (z/b) ratio was 0.4. As a result, it was seen that the choice of the end and middle width of the lock is very important for the load-carrying capacity. Besides, the fact that maximum damage loads change with the increase in (b/w) ratio indicates the importance of the lock width.

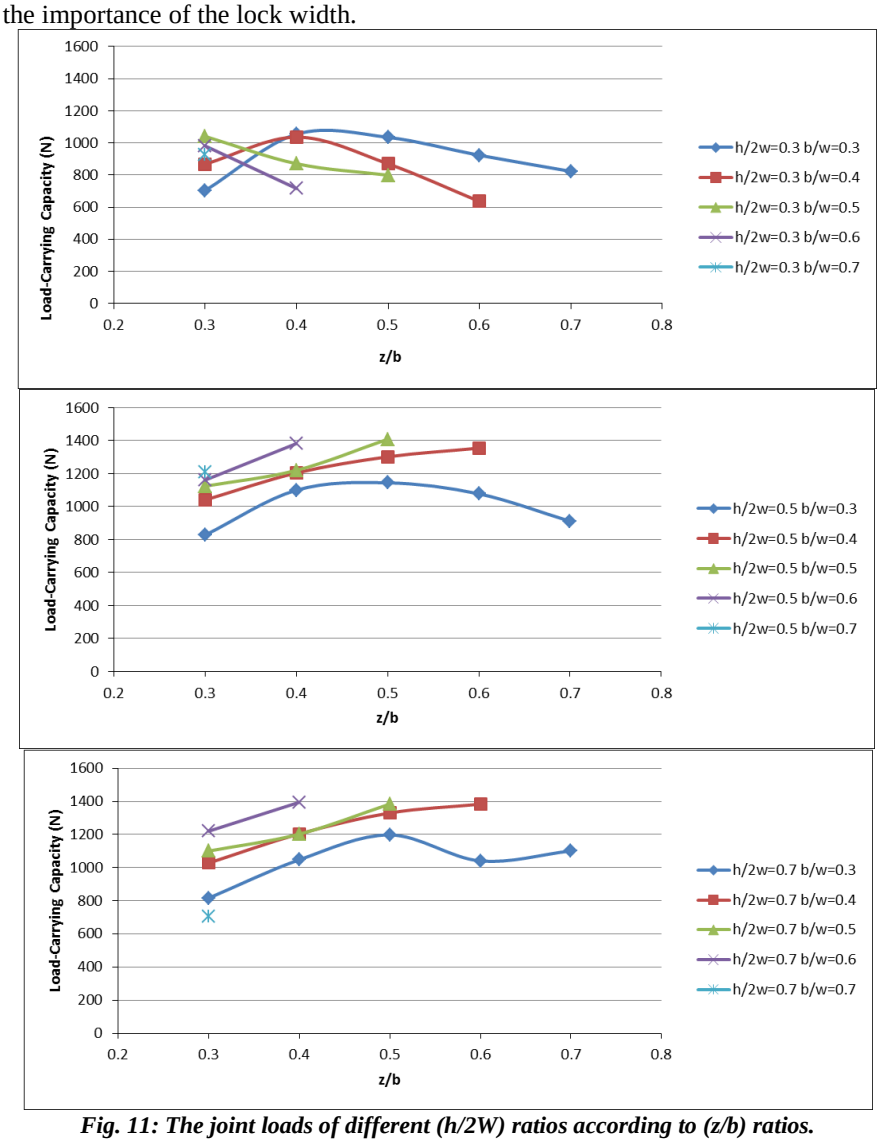

Fig. 11: The joint loads of different (h/2W) ratios according to (z/b) ratios.

Figure 11 examines the effects of the parameters at which maximum joint loads were achieved on the lock dimensions. Accordingly, the changes in the maximum damage loads of the locked joints and the forms of the damage for different lock lengths are shown in Figure 12. As can be seen in the figure, for the lock length h/2W= 0.5, the damage load was maximum. In this study, therefore, the lock length h/2W= 0.5 was particularly dealt with and analyzed for the three-point bending.

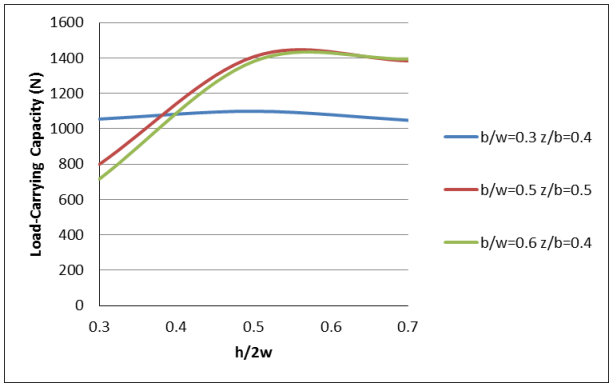

Fig.12:(a)

(b)

Fig. 12: The changes in the maximum damage loads of the locked joints and the forms of the damage for different lock lengths.

The changes in the load-carrying capacities of the joints with the lock joint elements made from the composite plate are shown in Figure 13 for the lock length (h/2W) = 0.5. As the ratio of the lock width to the width of the specimen increases, lock displacement also increases during the maximum load amount. However, it was understood from the experiments that after the 0.5 value, the increases were small and almost the same. It was found out that when the ratio of lock width to the width of the specimen (b/W) was 0.5, the specimen had the maximum bending load when compared with the other specimens at all the values of the (z/b) ratios. When the load-carrying capacities of the specimens whose (z/b) ratio was 0.3 were compared with those of the others, it was observed that (b/W) ratio increases till it was 0.5 and it remained almost at the same value after this value. Similarly, when the load-carrying capacities of the samples whose (z/b) ratio was 0.5 were compared with those of the others, it was observed that (b/W) ratio increases till it was 0.5.

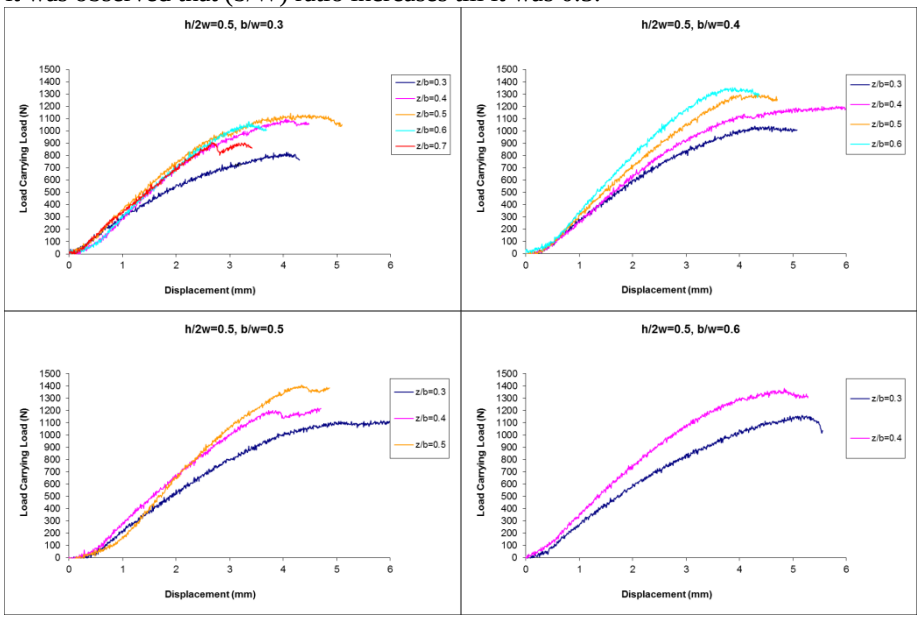

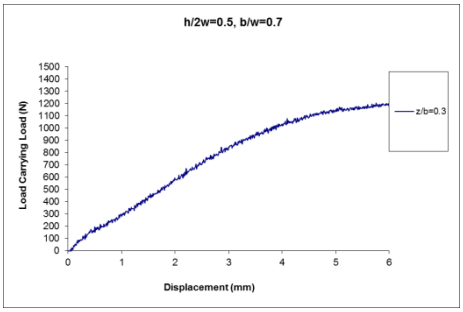

Fig. 13: The load-carrying capacities of the joints with the lock joint elements for the lock length (h/2W)=0.5.

According to the analyses, maximum joint load was observed when (b/W) ratio was 0.5 and (z/b) ratio was 0.5. The joint displacements acquired at three-point bending loadings indicate the deflection amounts of the specimens under these loadings. Maximum deflection amounts were determined as 4 mm on average when (b/W) ratio was on the increase until 0.6 and at different (z/b) values. However, when (b/W) ratio was 0.6 and 0.7, maximum deflection amounts were determined as 5 mm on average because the locks had big geometry.

To understand the latest cases of the damage shapes that may occur on the composite locked joints, after the bending experiments reached the maximum damage loads, they were continued until the load-carrying capacities fell down. Figure 14 shows the damage shapes of the composite locked joints made at the different values of geometric ratios of (b/W)-(z/b) and fixed 0.5 (h/2W) ratio that occurred in the experiments. Because of the three-point bending load, the upper part of the lock is exposed to compression loading and the lower part is exposed to the tensile loading. As can be seen in the figure, shear damages were observed on the lower end of the lock in particular when the (z/b) ratio was low. When the (z/b) ratio was high, damages were observed to have occurred together with the specimen first of all.

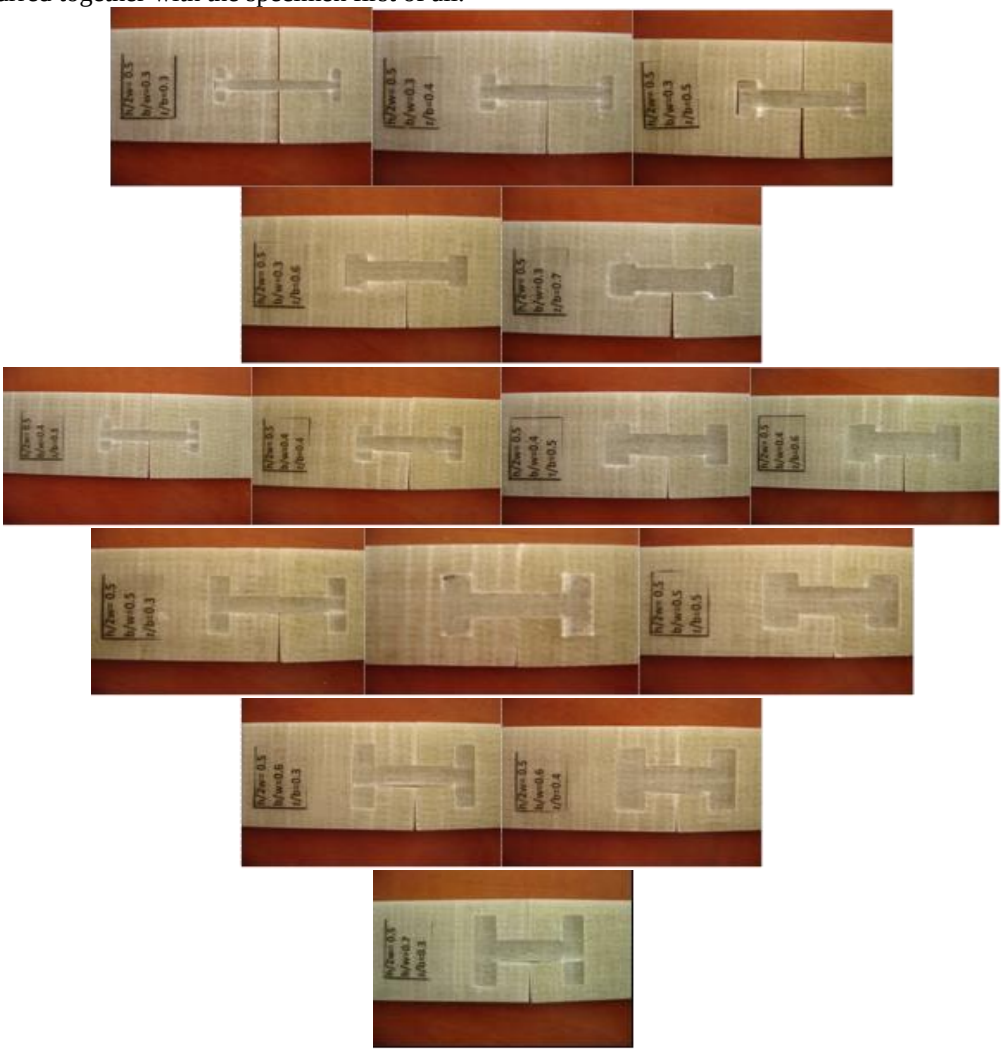

Fig. 14: Damage shapes of the composite locked joints for fixed 0.5 (h/2W) ratio.

Numerical optimization of the jointing element

Since the most optimum values were experimentally obtained when h/2W ratio was 0.5, this ratio was taken as the basis in the numerical study. Figure 15 shows the stress values that occurred along Way 1 and Way 2 at different ratios of z/b under the geometry parameters of h/2W=0.5 and b/W=0.5. It is seen from Figure 15 that Way 1 and Way 2 stress values of the joints at the ratios of z/b=0.3 and z/b=0.4 are very high. The stress distribution of Way 1 and Way 2 at the joint with the z/b ratio of 0.4 is similar to the joint with the z/b ratio of 0.3 but its stress values were found as lower. The stress values that occurred at the joints with the z/b ratio of 0.5 were found as lower than the ones that were obtained at the other z/b ratios. It is expected that higher load-carrying capacity will be obtained from the geometries with lower stress values. As a result, it was determined that the joint with the z/b ratio of 0.5 would have a higher damage load than the other models.

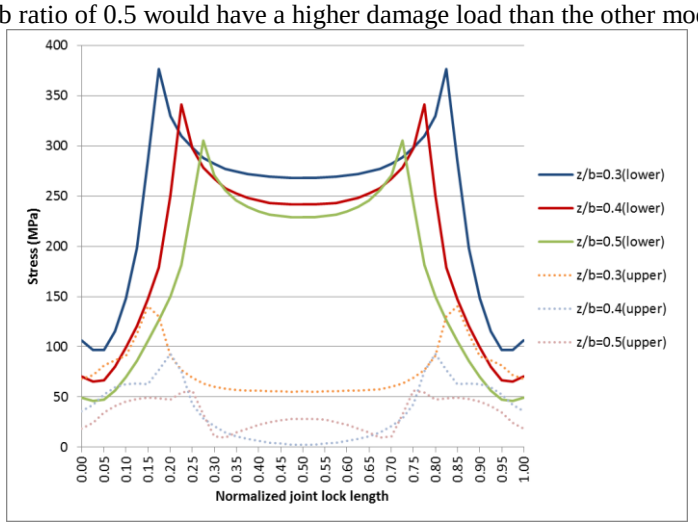

Fig. 15: Stress values that occurred along Way 1 and Way 2 at different ratios of z/b under the geometry parametres of h/2W=0.5 and b/W=0.5.

With the Abaqus finite elements program, the most proper lock joint element geometries were determined for the z/b ratios at each b/W. At the b/W ratio of 0.5 and z/b ratio of 0.5, the stress values obtained are low; the difference between the maximum values on Way 1 and Way 2 is small, and the stress distribution is homogeneous. Therefore, the joint at these ratios was determined to transmit the load better. Thus, it is assumed that this joint lock will be damaged later than the others. For these reasons it was determined that the joint at these ratios is optimum. Experimental studies were supported by this stress analysis.

Failure Analysis

The failure analysis of the specimen with best load-carrying capacity as obtained from the stress analyses conducted by using the finite elements method was conducted for the specimen that had got the Hashin Failure Criteria of h/2W=0.5-b/W=0.5 and z/b=0.5 ratios. In this way, the results obtained from the stress analysis were propounded in a more clear way. It was determined accordingly that damage had occurred in the regions where stress values were high on the composite structure. Moreover, the determination of the damage force that caused the damage was obtained for the tensile and compression cases of the matrix and the fiber components, and shown in Figure 16. Damage loads were found by bringing the damage index value obtained from the finite elements analysis to the value of 1.

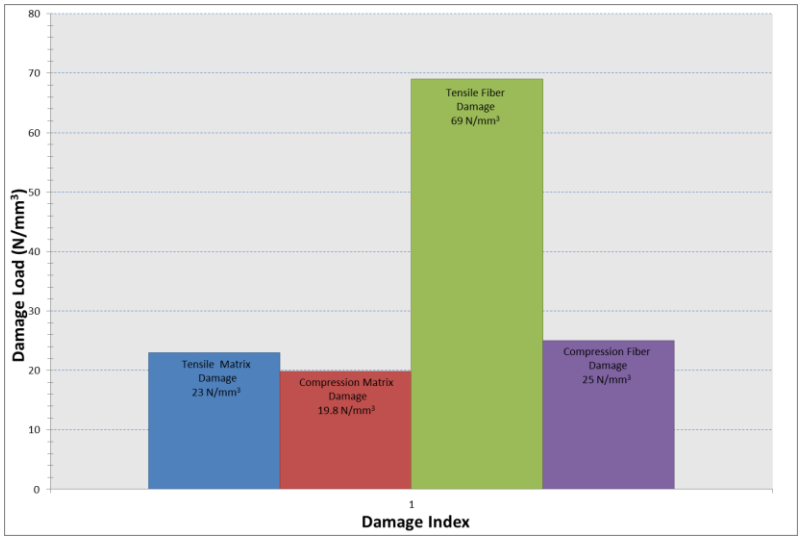

Fig. 16: Damage index of h/2W=0.5-b/W=0.5 and z/b=0.5 ratios.

Because of the fact that damages on the laminated semi specimen jointed and modelled in the Abaqus finite elements program first occurred on the joint lock, the first damage loads both for the fiber and matrix of the composite layers making up the joint lock were given in Table 3.

Table 3. First damage loads and damage index

Initial damage loads (N/mm^3)	Compression Matrix Damage	Tensile Matrix Damage	Compression Fiber Damage	Tensile Fiber Damage
19.8	1	0.792	0.629	0.088
23	1.316	1	0.864	0.118
25	1.459	1.266	1	0.139
69	8.679	9.828	1.4	1

Now that the volume of the bending the tip of the pin on which bending load is applied is 27.5 mm^3, the first damage was obtained as matrix compression damage at about 544.5 N. These damage indices belong to the layer that was first damaged on the composite specimen. Given that composite layers are eight, it was determined with the experiment conduce that the damage that occurred on this single layer did not affect the whole structure. Therefore, it was determined when the cross-section analysis was made that the first compression damage occurred on the layer in the center and as the amount of load increased, the damage advanced from the center to the outer surface of the specimen. As the other damage loads, the first matrix tensile damage was found as 632.5 N, the first fiber compression damage as 687.5 N and the first fiber tensile damage as 1897.5 N.

Table 4 shows the damage indices occurring on the maximum damage load of the joint lock. The load value is nearly same with the load obtained from experiment. This shows the numerical analysis is supported by experimental analysis.

Table 4. The damage indexes occurring on the maximum damage load of the joint lock

Experimental Load (N/mm^3)		Compression Matrix Damage	Tensile Matrix Damage	Compression Fiber Damage	Tensile Fiber Damage
50	Maximum damage index	2.947	4.849	3.347	0.542
	Damage index of whole composite structure	1	0	0.3	0

Figure 17 shows the tensile distributions and values for the tensile and compression cases of the matrix and fiber components in the Hashin failure analysis for the joint lock with the h/2W ratio of 0.5, b/W ratio of 0.5 and z/b ratio of 0.5. It is seen from Figure 17 (a) that matrix tensile damage occurred on the internal corner of the joint lock at 1375 N (50 N/mm^3) loading. It is seen from Figure 17 (b) that matrix compression damage occurred on the internal corners of the joint lock, on its arms and on the semi specimen on which bending the tip of the pin force was applied. In Figure 17 (c), because fiber tensile damage was subjected to the tensile stress, it appeared to have occurred on the middle body of the joint lock and on the semi specimen. Fiber compression damage occurred on the internal corners of the joint lock. As can be understood from Table 4 and Figure 17, matrix compression damage preceded the fiber compression damage.

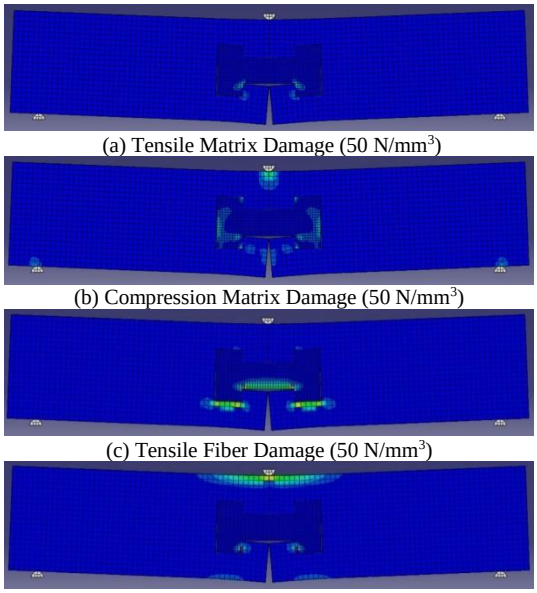

(a) Tensile Matrix Damage (50 N/mm^3)

(b) Compression Matrix Damage (50 N/mm^3)

(c) Tensile Fiber Damage (50 N/mm^3)

(d) Compression Fiber Damage (50 N/mm^3)

Fig. 17: Failure analysis under 50 N/mm3 load and at h/2W=0.5-b/W=0.5-z/b=0.5 ratios.

IV. CONCLUSION

In this study, three-point bending test and numerical analysis by using the program package ABAQUS was carried out in the different geometric parameters of the jointing element with profile I.

- Maximum stresses appeared to have occurred on the middle and internal corners of the lock joint element.
- The stress results of the joint lock element at different h/2W ratios were found. For each ratio, stress values were found and the most proper parameter was found as h/2W=0.5.
- As the z/b ratio increased, the load-carrying capacity of the lock joint element increased.
- I joint element whose load-carrying capacity whose load-carrying capacity will be damaged the latest and whose maximum tensile homogeneous distribution is the most proper was found as the geometry with the h/2w ratio of 0.5, b/w ratio of 0.5 and z/b ratio of 0.5.
- It was seen from the experiments that the choice of the lock end and middle width is very important for the load-carrying capacity.
- It was determined in the experiments that shear damages occurred on the lower end part of the lock in particular when the z/b ratio was small. However, when the (z/b) value was high, the damages first occurred with the matrix as matrix crush.
- It was determined that the first damage load value obtained from the experiments and the first damage load value obtained from Abaqus finite elements program are quite close to each other. Also the results were found to be in harmony.
- It was determined that the maximum tensiles of the fiber compression and matrix tensile damages, except for the matrix compression damage, occurred on the lock joint element and semi specimen.
- It has been concluded that considering that the first damage will occur on the jointing element with profile I before the jointed composite specimens and consequently composite structures are totally damaged, jointed composite structures can be made to work longer through the repairment of the jointing element.

V. ACKNOWLEDGEMENTS

The authors would like to express their appreciation to the TUBITAK, Turkey, and Project No: 110M250 for providing financial support for this study.

VI. REFERENCES

[1] M. Topcu, G. Altan, E.Ergun, “An Experimental Investigation on Damage Loads of Butterfly Joints in Composite Structures,” Advanced Composites Letters, 16(6), 197-204, 2007.

[2] Y. Zhou, H. Yazdani-Nezhad, M.A. McCarthy, X. Wana, C. McCarthy, “A study of intra-laminar damage in double-lap, multi-bolt, composite joints with variable clearance using continuum damage mechanics,” Composite Structures, 116, 441–452, 2014.

[3] E.A. Diler, C. Ozes, G. Neser, “Effect of T-Joint geometry on the performance of a GRP/PVC sandwich system subjected to tension,” Journal of Reinforced Plastics and Composites, 28, 49-58, 2009.

[4] P.A. Sharos, B. Egan, C.T. McCarthy, "An analytical model for strength prediction in multi-bolt composite joints at various loading rates," Composite Structures, 116, 300-310, 2014.
[5] J.H. Kim, B.J. Park, Y.W. Han, "Evalution of fatigue characteristics for adhesively-bonded composite stepped lap joint," Composite Structures, 66, 69-75, 2004.
[6] C. Yang, H. Huang, J.S. Tomblin, W. Sun, Elastic-plastic Model of Adhesive-bonded Single-lap Composite Joints, Journal of Composite Materials, 38, 293-302 (2004).
[7] J.H. Kweon, J.W. Jung, T.H. Kim, J.H. Choi, D.H. Kim, "Failure of carbon composite-to-aluminum joints with combined mechanical fastening and adhesive bonding," Composite Structures, 75, 192-198, 2006.
[8] G. Li, J.H. Chen, M. Yanishevsky, N.C. Bellinger, "Static strength of a composite butt joint configuration with different attachments," Composite Structures, 94, 1736-1744, 2012.
[9] K. Song, J.Y. Choi, J.H. Kweon, J.H. Choi, K.S. Kim, "An experimental study of the insert joint strength of composite sandwich structures," Composite Structures, 86, 107-113, 2008.
[10] K.S. Kim, Y.M. Yi, G.R. Cho, C.G. Kim, "Failure prediction and strength improvement of uni-directional composite single lap bonded joints," Composite Structures, 82, 513-520, 2008.
[11] A. El Mahi, A. Bezazi, "Describing the flexural behaviour of cross-ply laminates under cyclic fatigue," Applied Composite Materials, 16, 33-53, 2009.
[12] A. Megueni, A. Tounsi, E. Adda Bedia, "Evolution of the stress ıntensity factor for patched crack with bonded hygrothermal aged composite repair," Materials and Design, 28, 287-293, 2007.
[13] J.H. Choi, Y.J. Chun, "Failure load prediction of mechanically fastened composite joints," Journal of Composite Materials, 37, 2163-2177, 2003.
[14] G. Altan, M. Topcu, "Experimental and numerical assessment of the improvement of the load-carrying capacities of butterfly-shaped coupling components in composite structures," Journal of Mechanical Science and Technology, 6, 1245-1254, 2010.
[15] V.R.L. Kumar, M.R. Bhat, C.R.L. MurthyL, "Experimental analysis of composite single-lap joints using digital image correlation and comparison with theoretical models," Journal of Reinforced Plastics and Composites, 32, 1858-1876, 2013.
[16] T.H. Kim, J.H. Kweon, J.H. Choi, "An experimental study on the effect of overlap length on the failure of composite-to-aluminum single-lap bonded joints," Journal of Reinforced Plastics and Composites, 27, 1071-1081, 2008.
[17] D.W. Seo, J.K. Lim, "Tensile, bending and shear strength distributions of adhesive-bonded butt joint specimens," Composites Science and Technology, 65, 1421-1427, 2005.
[18] J.W. Nader, H.J. Dagher, R. Lopez-Anido, "Size effects on the bending strength of fiber-reinforced polymer matrix composites," Journal of Reinforced Plastics and Composites, 30, 309-316, 2011.
[19] M. Dawood, E. Taylor, S. Rizkala, "Two-way bending behaviour of 3-D GFRP sandwich panels with through-thickness fiber insertions," Composite Structures, 92, 950-963, 2010.
[20] S.M.R. Khalili, A. Shokuhfar, S.D. Hoseini, M. Bidkhori, S. Khalili, R.K. Mittal, Experimental study of the influence of adhesive reinforcement in lap joints for composite structures subjected to mechanical loads, International Journal of Adhesion & Adhesives, 28, (2008) 436- 444.
[21] A. Roy, C. Mabru, J.L. Gacougnolle, P. Davies, "Damage mechanisms in composite/composite bonded joints under static tensile loading," Applied Composite Materials, 4, 95-119, 1997.
[22] S.B. Baştürk, M. Tanoğlu, "Development and mechanical behaviour of FML/Aluminium foam sandwiches," Applied Composite Materials, 20, 789–802, 2013.
[23] S.M. Radhakrishnan, B. Dyer, M. Kashtalyan, A.R. Akisanya, I. Guz, C. Wilkinson, "Analysis of bolted flanged panel joint for GRP sectional tanks," Applied Composite Materials, 21, 247-261,2014.